Magnetic Susceptiblity Induced MR Signal Frequency Shift in White Matter - Experimental Comparison Between Lorentzian Sphere and Generalized Lorentzian Approaches

Jie Luo[1], Xiang He[2], and Dmitriy A Yablonskiy[3,4]

[1]Chemistry, Washington University in St.Louis, St. Louis, MO, United States, [2]University of Pittsburg, [3]Radiology, Washington University in St.Louis, [4]Physics, Washington University in St.Louis, United States

Introduction: Phase images obtained by gradient echo MRI provide enhanced contrast of the brain anatomy [1]. Possible origins of the phase/frequency contrast such as the magnetic susceptibility [2, 3] and the water-macromolecule exchange effects [4, 5] have been discussed. To describe the influence of tissue magnetic susceptibility χ on a corresponding MR signal frequency shift, Δf, a proper relationship between these two values should be established. For isotropic structures such a relationship is provided by a Lorenztian sphere approximation: $\Delta f / f_0 = (4\pi/3)\chi$ [6], where f_0 is a base Larmor frequency. However, this relationship failed to explain the absence of phase contrast between WM and CSF [2]. Accordingly, it was proposed in [7] that for anisotropic cellular structures such as axons in WM a Generalized Lorentzian Approach should be used to account for the longitudinal distribution of magnetic susceptibility inclusions (myelin sheath, neurofilaments, etc.) at the cellular and sub-cellular levels. In this study, we are using ex vivo rat optic nerve as a representative white matter model to validate this theory.

Material and Methods: Rat optic nerves were harvested from euthanized rats, and subsequently fixed with 10% formalin. They were then suspended in the NMR tube, filled with 10% formalin fixative, parallel to the tube axis. Experiments were performed on a Varian DirectDrive™ 4.7T MR scanner using a 1.5 cm diameter surface transmit/receive RF coil. Data was collected using 2D multi-echo gradient echo sequence with 8 echoes, 1mm thick slice with 75x75 μm^2 in plane resolution. TR = 170 ms, first TE = 7 ms, echo spacing = 9 ms, FA = 30 deg, imaging matrix 128x128, 50 averages. The tube was first oriented parallel to the magnetic field B_0 and then rotated four times to perpendicular orientation. Localized shimming was performed on an imaging slice achieving linewidth ~5 Hz. For each rotation, imaging plane was perpendicular to the NMR tube and the optic nerve.

Frequency shift around optic nerve: The in-plane frequency shift distribution due to the presence of the nerve is defined by Eq.[1], where χ_e is the magnetic susceptibility of formalin solution, α- the angle between magnetic field B_0 and nerve direction, θ - an angle in the imaging plane, r – distance from the nerve center and r_0 – nerve radius. Maximum frequency shift outside the nerve was observed when α=90

$$(\Delta f / f_0)\big|_{ext} = 2\pi(\chi - \chi_e)\sin^2\alpha(r_0/r)^2\cos(2\vartheta) \quad [1]$$

Frequency shift inside optic nerve: Under Lorentzian sphere approximation, this frequency shift would be given by Eq.[2]. However, the result is different under Generalized Lorentzian approach [7] as described by Eq.[3]. Here the magnetic susceptibility of the optic nerve is separated into two components $\chi = \chi_L + \chi_i$ that represent contribution from the longitudinal (neurofilaments, myelin sheath) and isotropic (cytoplasm) structures. While both components contribute to the external frequency shift, only isotropic susceptibility, χ_L, contributes to the frequency shift inside of the nerve. Testing the difference between Eqs. [2] and [3] under Eq. [1], allows distinguishing between Lorentzain sphere and Generalized Lorentzian approaches.

$$\Delta f / f_0\big|_{\text{int}} = -2\pi(\chi - \chi_e)\sin^2\alpha + (4\pi/3)(\chi - \chi_e) \quad [2]$$

$$\Delta f / f_0\big|_{\text{int}} = -2\pi(\chi_i - \chi_e)\sin^2\alpha + (4\pi/3)(\chi_i - \chi_e) \quad [3]$$

Results and Discussion: Figure on the right show magnitude (a and b) and corresponding phase (c and d) images of the optic nerve (dark circle, also shown in red on d) and surrounding formalin obtained at two orientations: 0° (upper row) and 90° (lower row). Frequency distribution outside of the nerve is uniform in parallel orientation and displays dipolar pattern in all other cases. The frequency of the surrounding media is obtained by averaging around the nerve along the blue dotted line Fig. d) so that frequency bias created by the optic nerve is excluded. The angular dependency of the frequency shift inside optic nerve - frequency shift versus $\sin^2\alpha$– is shown in Plot A. The result from fitting Eq.[1] to frequency distribution surrounding optic nerve, is illustrated in Plot B. If the Lorenzian approximation would be valid, the magnitude of the slopes in Plots A and B would have been the same, which contradicts with our measurement: the slope is (0.0555 ± 0.0026) ppm from Plot A, and (-0.0628 ± 0.0009) ppm from Plot B. Further, the linearity of both curves is very good, hence the $\sin^4\alpha$ term, as proposed in [8] to describe the susceptibility anisotropy, would be very small according to our data. To the contrary, Generalized Lorentzian approach provides a consistent explanation of our observations. The estimated $\chi_i - \chi_e$ and χ_L is (8.8±0.4) and (1.2±0.5) ppb, respectively. Also note that from Eq.3, the intercept of Plot A should be (-2/3) of its slope. The deviation from the predicted value (0.037 ppm) can be attributed to the water-macromolecule exchange effect [4, 5] .

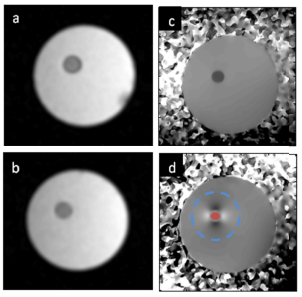

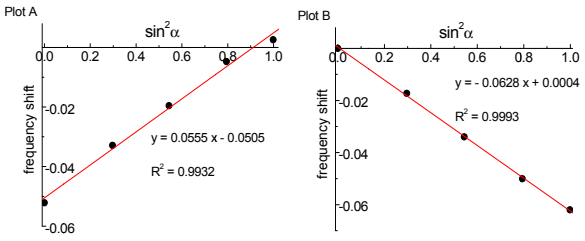

Conclusion: We have demonstrated that the Generalized Lorentzian Approach provides satisfactory explanation of the angular dependence of the phase contrast in longitudinal structures such as axons in white matter while usually assumed Lorentzian Sphere Approximation fails. Also, $\sin^4\alpha$ behavior is hardly observed for the angular dependency of frequency shifts.

References: **1**. Duyn and Koretsky, Curr Opin Neurol, 2011, 24, 386. **2**. Duyn, et al., PNAS, 2007, 104, 11796. **3**. Liu, MRM, 2010, 63, 1471. **4**. Zhong, et al., Neuroimage, 2008, 40, 61. **5**. Luo, et al., JMR, 2010, 202, 102. **6**. Chu, et al., MRM, 1990, 13, 239. **7**. He and Yablonskiy, PNAS, 2009, 106, 13558. **8**. Lee, et al, Neuroimage, 2011, 57, 225.